Polymers with Palladium Nanoparticles as Active Membrane Materials

J. Yu,[1] R. Y. F. Liu,[1] B. Poon,[1] S. Nazarenko,[1] T. Koloski,[2] T. Vargo,[2] A. Hiltner,[1] E. Baer[1]

[1]Department of Macromolecular Science and Center for Applied Polymer Research, Case Western Reserve University, 10900 Euclid Avenue, Cleveland, Ohio 44106
[2]Integument Technologies, Incorporated, Tonawanda, New York 14150

ABSTRACT: A new *in situ* infusion method was used to incorporate small amounts ($\sim$ 1 wt %) of metal and metal oxide particles into a polymer matrix. Nanosized particles were observed by both transmission electron microscopy and atomic force microscopy. Oxygen (O_2) and carbon dioxide (CO_2) transport properties of the infused materials were investigated using a dynamic diffusion approach in which both testing and purge gases can be controlled. It was discovered that trace amounts ($\sim$ 2%) of hydrogen (H_2) in the purge gas were sufficient to considerably reduce the O_2 flux of FEP films infused with palladium (Pd) nanoparticles, up to a 200-fold decrease. In contrast, H_2 essentially had no effect on the transport of CO_2. The generality of the remarkable reduction in oxygen flux was also demonstrated with films of PP, LLDPE, PET, and nylon 6,6 infused with Pd nanoparticles. This oxygen-scavenging effect became more pronounced at lower oxygen concentrations. The catalytic role of Pd in the reaction of O_2 and H_2 and the enormous surface area provided by the dispersed nanoparticles were responsible for this highly efficient oxygen-scavenging effect. © 2004 Wiley Periodicals, Inc. J Appl Polym Sci 92: 749–756, 2004

Key words: selectivity; nanoparticles; catalysis; separation techniques; oxygen permeability

INTRODUCTION

Particles in the nanometer-size range serve as the bridge between atoms/molecules and bulk materials. Because of their quantum-scale dimensions,[1] nanoparticles exhibit properties different from those of the bulk.[2–5] As a result of their unique properties, numerous efforts have been made to disperse nanoparticles in polymers to enhance or modify electrical,[6–8] optical,[9,10] catalytic,[3,11] and mechanical[12] properties. For example, it has been reported that dispersion of fumed silica nanoparticles in a polymeric membrane enhances both the permeability and selectivity for large organic molecules over small permanent gases.[13] Usually, membrane permeability and selectivity cannot be increased simultaneously. It may even be possible to create reactive membranes that combine both catalytic and separation functions using nanoparticles.[3,14,15]

The surface area of nanoparticles is 2 to 4 orders of magnitude higher than that of more conventional micron-scale particles.[16,17] To use this high surface area in a polymer matrix, very good dispersion is required. Most inorganic nanoparticles are typically in the form of agglomerates before they are dispersed. Because such nanoparticles adhere strongly to each other, it is difficult to separate these agglomerates into individual particles and disperse them uniformly in a polymer matrix.[17] This compromises the potential property enhancement that the nanoparticle would have afforded.[18,19] The two most common approaches to dispersing nanoparticles are direct blending and *in situ* polymerization. Direct blending can be performed in the melt or in solution. Dispersion largely depends on the shear force between particle and polymer melt or solution. Although this approach is attractive, it is often unsuccessful in obtaining good dispersion of nanoparticles.[19] Chemical treatment of the nanoparticles to increase compatibility with the hydrophobic polymer can improve dispersion to some extent.[20] It has been shown that nanoparticles are more easily dispersed in a monomer solution that is subsequently polymerized with the nanoparticles *in situ*.[21,22] However, the particular requirements of this approach are restricted to certain polymerization procedures.

Recently, an infusion approach was developed that uses the inherent free volume of the solid polymer to obtain a dispersion of inorganic metal or metal-oxide nanoparticles.[22–24] In this method, a solid polymer is evacuated and a volatile precursor is infused into the evacuated free volume. Subsequent thermal or chem-

TABLE I
Polymeric Materials with Infused Nanoparticles Used in This Study

Polymer	Nanoparticles	Metal content (wt %)
	1XPd/5XPd[a]	0.41/0.83
FEP[b]	1XPt	1.04
	3XAu	0.31
	3XAg	0.36
PP[c]	1XPd	0.29
LLDPE[c]	1XPd	0.76
PET[c]	1XPd	0.70
Nylon 66[c]	1XPd	0.24

[a] Number indicates the number of infusion cycles.
[b] Commercial films.
[c] Films molded from the nanoparticle-infused pellets.

ical transformation of the precursor results in the formation of discrete nanoscale particles. Because most metals have volatile precursors, this method is amenable to metals and metal oxides. It requires only a metal precursor that can be volatized below the decomposition temperature of the polymer.[22–24] This method is also applicable to organic precursors. For example, monomers such as styrene can be infused and polymerized within the polymer free volume.[22–24] The infusion cycle can be repeated to increase the concentration of nanoparticles.

In this study, a new class of polymer–metal films containing nanoparticles were prepared using the infusion approach. The strong catalytic effect of various metal nanoparticles on the gas transport properties of fluorinated ethylene–propylene copolymer (FEP) and other polymer films is reported.

EXPERIMENTAL

Thermal gravimetric analysis (TGA)

The metal composition of polymer infused with nanoparticles was determined with a Perkin–Elmer TGA-7 (Perkin Elmer Cetus Instruments, Norwalk, CT). The sample purge was oxygen and the furnace purge was nitrogen. The temperature was increased from 100 to 700°C at 20°C/min to completely degrade the polymer.

Morphology study

The size of palladium (Pd) particles infused into FEP film was examined using atomic force microscopy (AFM). The sample was first microtomed at −100°C and then imaged using a Digital Instruments Nanoscope IIIa AFM (Santa Barbara, CA) operating in the tapping mode. Light tapping was used with a setpoint ratio of 0.75 to 0.85 and with a freely oscillating tip amplitude of 48 nm. To distinguish Pd particles from

FEP crystals, the tapping frequency was slightly increased from the freely oscillating tip resonant frequency. The particle size and concentration were also examined elsewhere using TEM.

Gas transport properties

The oxygen flux $J(t)$, at 0% relative humidity, 1 atm pressure, and 23°C, was measured with a Mocon Ox-Tran 2/20 (Minneapolis, MN).[25] The testing gas was either pure oxygen or dry air. The carrier gas was either pure nitrogen or nitrogen with 2% hydrogen. The carbon dioxide flux $J(t)$, at 0% relative humidity, 1 atm pressure, and 23°C, was measured with a Mocon Permtran C4/40. The testing gas was pure carbon dioxide. Again, the carrier gas was either pure nitrogen or nitrogen with 2% hydrogen.

RESULTS AND DISCUSSION

Particle concentration and morphology

In this study, several organometallic complex precursors were infused into a 10-mil commercial fluorinated ethylene–propylene copolymer (FEP) film. The precursor was then decomposed to create *in situ* metal nanoparticles.[22–24] To increase the metal content, the infusion process was repeated. Throughout this investigation, the amount of infused metal nanoparticles determined by TGA was less than 1 wt % (Table I). For example, the Pd concentration in FEP/Pd5X film

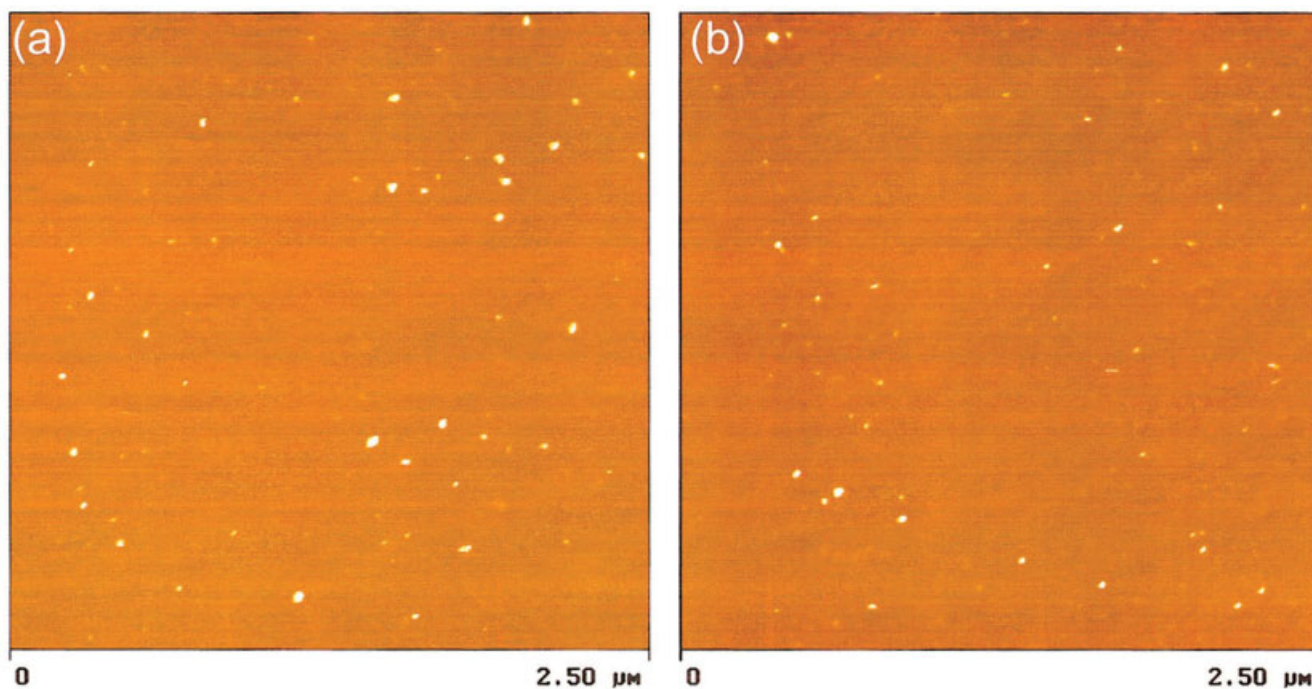**Figure 1** AFM phase image of FEP free-melted surface.

Figure 2 AFM phase images of the FEP film infused with Pd nanoparticles: (a) edge of the film; (b) center of the film.

infused five times was found to be 0.84 wt % (0.15 vol %).

The phase image of free-melted FEP observed in the AFM revealed a highly crystalline morphology. Short, densely packed, wormlike lamella 20–40 nm wide and 150–200 nm long were seen (Fig. 1). Because the resonant frequency of the AFM tip interacting with the metal nanoparticle is different from that of the polymer crystal, the tapping frequency was increased slightly to distinguish metal nanoparticles from poly-
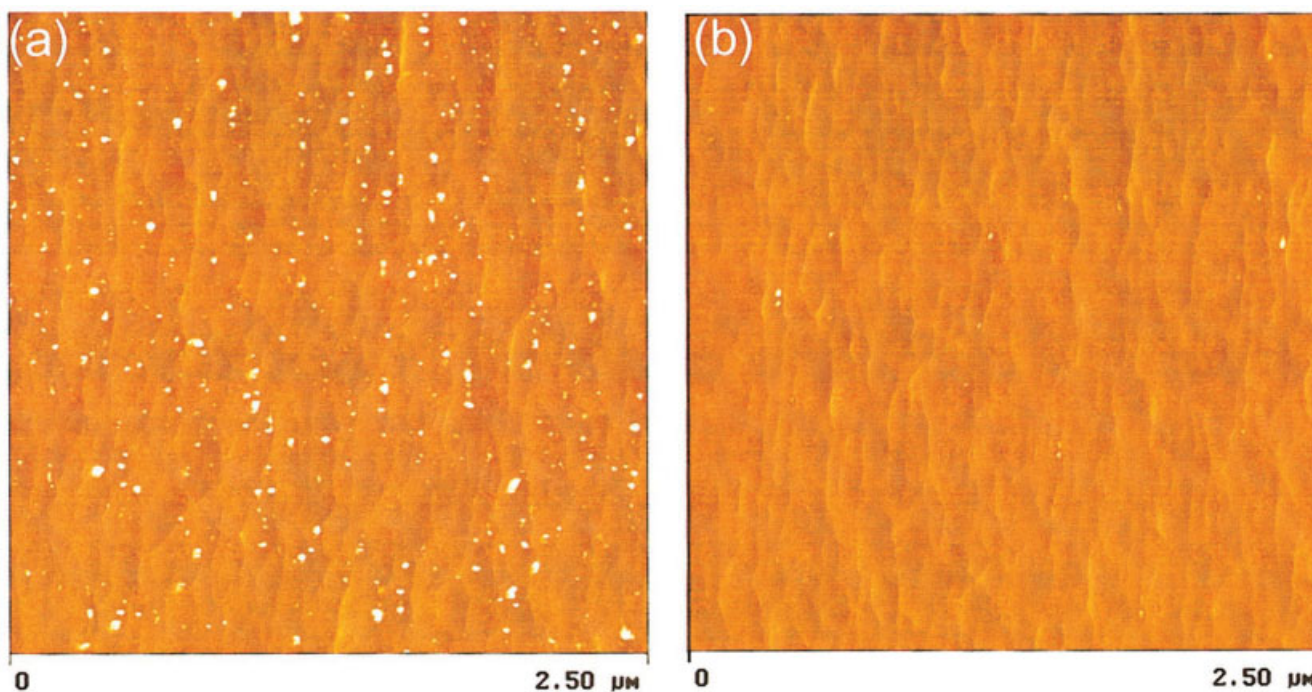

Figure 3 AFM phase images of the nylon 6,6 pellet infused with Pd nanoparticles: (a) edge of the pellet; (b) center of the pellet.
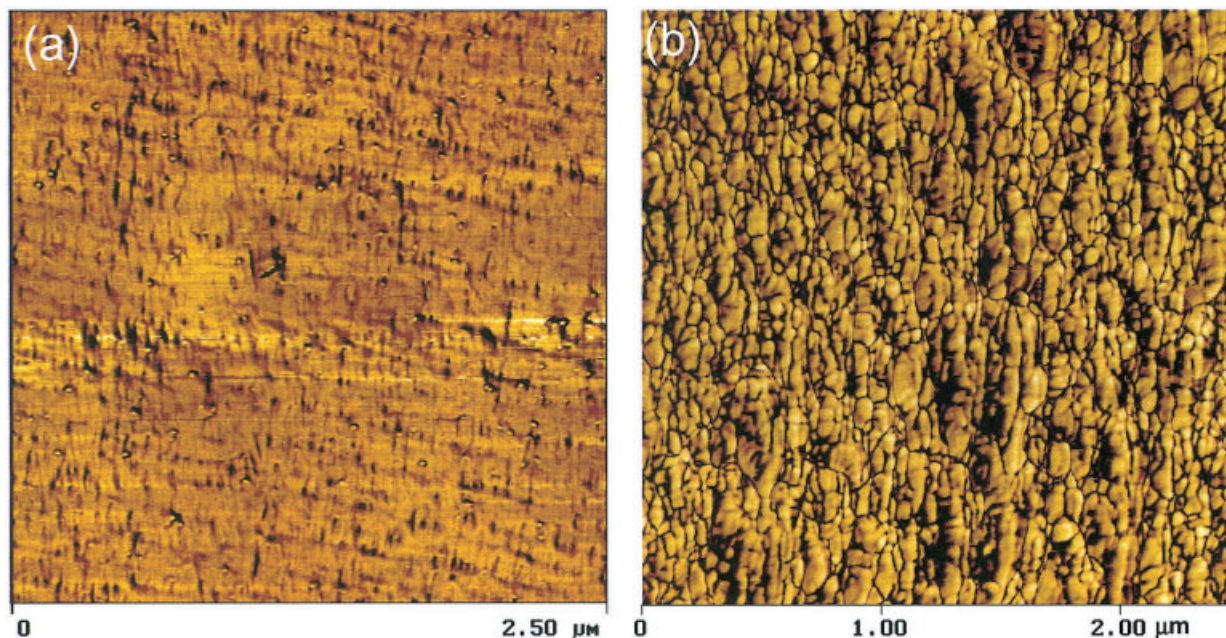
Figure 4   AFM phase images of the PET pellet infused with Pd nanoparticles: (a) edge of the pellet; (b) center of the pellet.

mer matrix. Fairly uniform nanoparticles about 10–40 nm in diameter (Fig. 2) were observed throughout the FEP/5XPd film, and particle density did not vary much through the thickness of the film.

This infusion approach was also successfully applied to various commercial polymer pellets. More particles were observed near the surface of the pellets in both nylon 6,6 and PET pellets (Figs. 3 and 4), which could be attributed to differences in the transport properties of precursors in various polymers during the infusion process.

The nanosized particle morphology in single and multiple (5X) Pd-infused FEP films was examined elsewhere using TEM (Fig. 5). Well-dispersed Pd nanoparticles of about 2–5 nm in diameter were observed. An increase in Pd nanoparticle size and concentration was obtained after multiple infusions. Examination of different cross sections showed that the particle concentration did not noticeably vary through

the thickness of the film. The smaller particle size determined from TEM (2–5 nm) compared to that determined by AFM (10–40 nm) can be attributed to the analytical microscopic procedures. Nevertheless, both microscopic techniques revealed that the nano-sized particles in the metal–polymer nanocomposites have large size distribution.

Gas transport properties

Gas transport measurements were used to probe the chemical activity of the infused nanoparticles. For the gas transport measurement, an inert purge gas was used to carry diffused gas to the sensor (Fig. 6). With pure nitrogen as the purge gas, the oxygen permeability of the FEP/Pd nanoparticle film was slightly lower than that of the FEP control film (Table II). An enhanced permeability effect reported previously[13] was not seen in our experiments. Instead, a decrease in
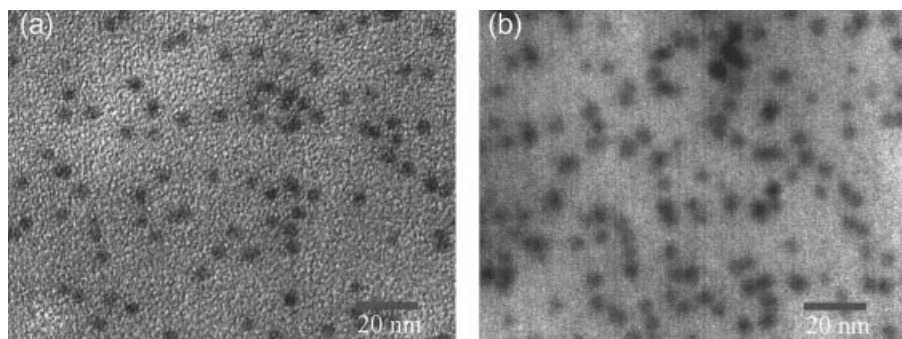

Figure 5   TEM images of single and multiple (5X) infused Pd–FEP films.
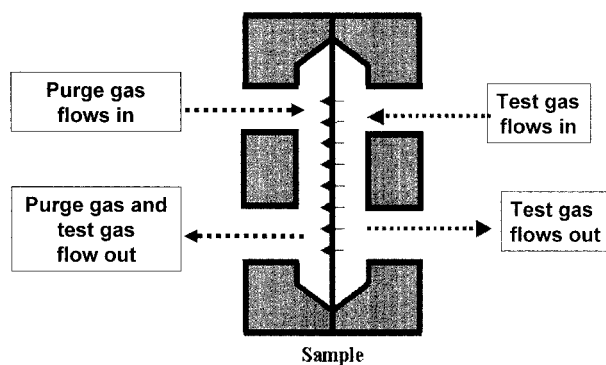
Figure 6 Dynamics in a gas diffusion cell.

permeability of 15% was measured, which could be attributed to the fact that the metal nanoparticles filled holes of free volume.

However, quite surprisingly, when 2% hydrogen was added to the purge gas, the oxygen permeability of FEP/Pd film was reduced by 2 orders of magnitude (Fig. 7, Table II). This very large oxygen-scavenging effect indicated that a chemical reaction occurred between oxygen and hydrogen that was catalyzed by Pd. To demonstrate the catalytic role of the Pd nanoparticles, FEP films infused with other metals were investigated. FEP film that was infused with gold and silver nanoparticles showed no catalytic effect (Fig. 8, Table II). To demonstrate the specificity of the chemical reaction to only oxygen gas, carbon dioxide permeability of FPE/Pd nanoparticle film was found to be essentially unaffected by 2% hydrogen in the purge gas (Table II).

FEP film is highly permeable to hydrogen gas and hydrogen diffuses rapidly from the purge stream into the film. It strongly adsorbs onto the Pd nanoparticles. Palladium hydrides of the form PdH_x ($0.1 < x < 0.7$) are known to form on the surface of Pd at 1 atm pressure and 25°C.[26,27] Sorbed hydrogen rapidly reacts with the diffusing oxygen to form water, thereby effectively scavenging oxygen from the permeant gas stream.

A recent study showed that hydrogen and oxygen react above 220 K at 1 atm on the Pd surface with formation of water.[28] The reaction is thought to proceed stepwise as follows:

$$O + H \rightarrow OH \qquad (1)$$

$$OH + H \rightarrow H_2O \qquad (2)$$

This reaction mechanism is depicted in Figure 9. The first reaction is slow and rate limiting; the second reaction is fast.[28,29] Water produced by the reaction diffuses out of the film into the gas streams. It is reported that water is desorbed immediately from Pd above 175 K.[28] If the water did not desorb, but remained sorbed to the Pd surface, a rough estimate indicates that the surface would be completely covered within 1 h. This fact is also supported by comparing the water-transport properties in FEP and FEP/5XPd; their permeability was found to be 1.99 and 2.02 $cm^3(STP)$ cm m^{-2} day^{-1} atm^{-1}, respectively, indicating that Pd did not affect the transport of H_2O. Thus the infused film constitutes a self-regenerating vehicle for removing oxygen from the gas stream.

The catalytic effect is strongly enhanced by the high surface area of the Pd nanoparticles. Assuming the particle size to be 25 nm, a 1 cm^2, 0.25-mm-thick FEP film, with 0.84 wt % Pd, would have 93 cm^2 of palladium surface. When the Pd concentration was reduced from 0.83 to 0.41 wt %, the oxygen-scavenging activity of Pd nanoparticles was still very effective (Table II).

The generality of the phenomenon was demonstrated by infusing other thermoplastic polymers with Pd nanoparticles. Pellets of polypropylene (PP), linear low-density polyethylene (LLDPE), and poly(ethylene terephthalate) (PET) were infused and compression molded into film. These polymers, infused with Pd

TABLE II
Effect of Infused Metal Nanoparticles on Gas Transport Properties of FEP Film

Material	Metal content (wt %)	O$_2$ transport		CO$_2$ transport	
		P^a (N$_2$ purge)	P (N$_2$ + 2%H$_2$ purge)	P (N$_2$ purge)	P (N$_2$ + 2%H$_2$ purge)
FEP	0.00	18.0	18.7	61.5	60.9
FEP-1X Pd	0.41	17.1	0.133	59.1	—
FEP-5X Pd	0.83	15.2	0.097	52.2	53.3
FEP-1X Pt	1.05	13.6	0.065	42.3	46.3
FEP-3X Ag	0.31	18.3	16.6	72.2	60.0
FEP-3X Au	0.36	17.5	19.8	69.2	58.7

^{a} P, cm^3[STP] cm m^{-2} atm^{-1} day^{-1}.
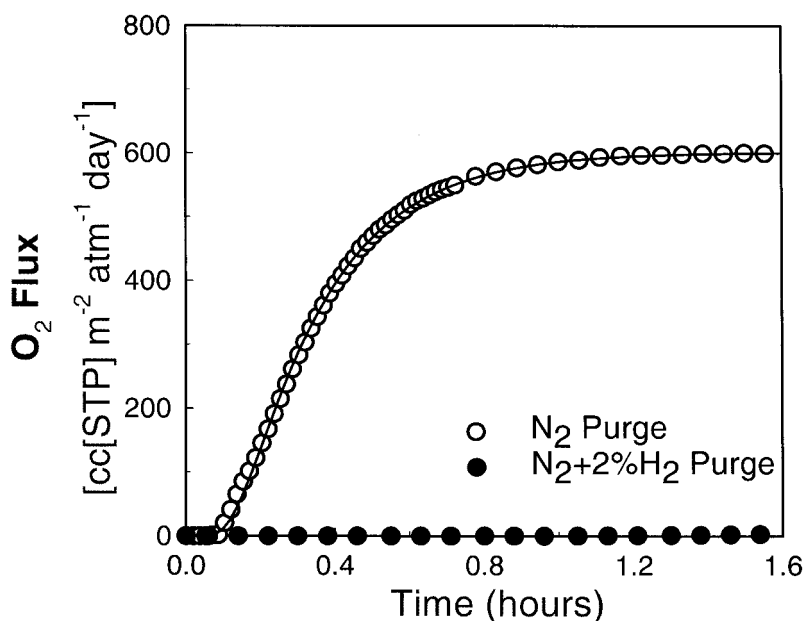
Figure 7   Effect of hydrogen in the purge gas on the oxygen transport properties of Pd-infused FEP film.

nanoparticles, also showed dramatic decreases in oxygen permeability. Infused PP films containing only 0.29 wt % Pd nanoparticles showed reduced oxygen permeability by more than 2 orders of magnitude. The oxygen permeability in both nylon 6,6 and PET films infused with Pd nanoparticles was almost undetectable (Table III). This demonstrates the feasibility of infusing polymer pellets that are routinely used in injection-molding and extrusion processes as a route to obtaining shapes and profiles with oxygen-scavenging and oxygen-separation properties. Because Pd is

an important catalyst for many chemical reactions and processes, the infused polymers can have an impact on many technologies in the chemical industry as well.

The driving force for gas transport is the pressure difference across the film. The partial pressure of oxygen in the permeant gas flow was reduced by replacing 1 atm oxygen with 1 atm air. Normalization of the measured oxygen flux to 1 atm oxygen pressure gave the permeability cited in Table IV. The presence of trace hydrogen (0.00005 vol %) in air was sufficient to reduce the oxygen permeability by 20% even with a
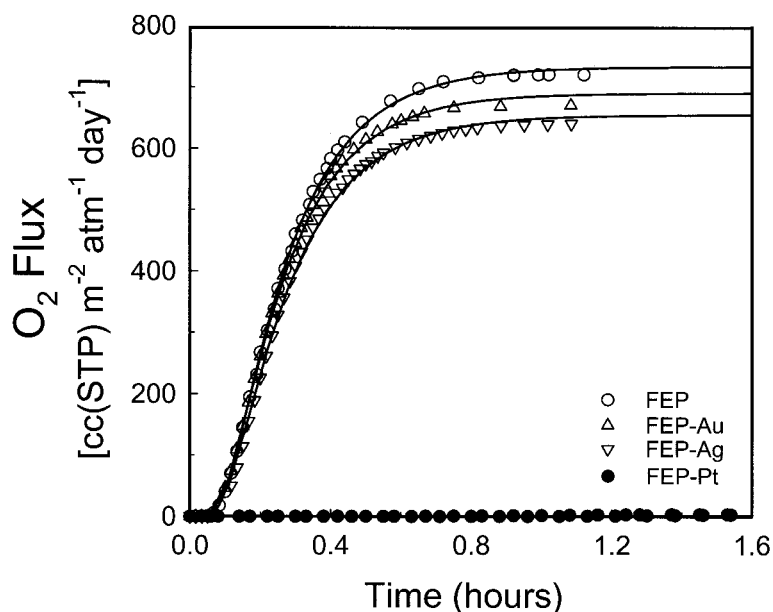

Figure 8   Oxygen transport through infused FEP film with nitrogen and hydrogen purge.
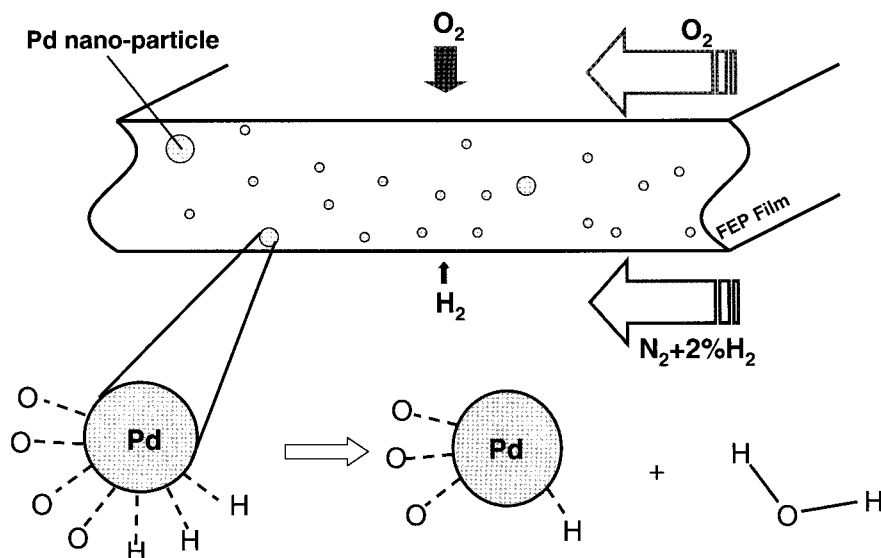
Figure 9 Reaction of oxygen and hydrogen in FEP–Pd film catalyzed by Pd nanoparticles.

pure nitrogen purge. With 2% hydrogen in the purge, the oxygen permeability in air at 1 atm was lower than the permeability of pure oxygen at 1 atm. Thus FEP/Pd film became more efficient for oxygen removal as the oxygen flux decreased. Membrane separation of oxygen and nitrogen has inherently low selectivity because of the similarity in molecular size. The relatively high nitrogen permeability of FEP and the efficiency of oxygen scavenging by the Pd nanoparticles suggest that FEP/Pd membranes containing nanoparticles can be used for separating high-purity nitrogen (>99.5%) from air.

CONCLUSIONS

Polymer films with nanoparticles were successfully fabricated by a unique infusion technology. Nanoparticles with large size distributions between 5 and 40 nm were observed by both AFM and TEM. Commercial thermoplastic polymers such as FEP, PP, LLDPE, PET, and nylon 6,6 were all successfully infused with various metal and metal-oxide nanoparticles.

Films containing less than 1 wt % Pd and Pt nanoparticles reduced the oxygen flux by 2 orders of magnitude when only traces of hydrogen were in the nitrogen carrier gas. These highly selective films could produce nitrogen of high purity (>99.5%) from air. Also, the catalytic role of Pd and Pt, coupled with the enormous surface area which is a characteristic of nanosized particles, gave a highly effective oxygen-scavenging system. The catalytic efficiency of these nanoparticles was independent of the chemical nature of the polymers.

TABLE III
Effect of Pd Nanoparticle on O_2 Transport
Properties of Various Polymers[a]

Material	Metal content (wt %)	N_2 purge P_1	N_2 + 2%H_2 purge P_2	P_1/P_2
PP	0.00	5.78	5.89	1.0
FP-Pd	0.29	7.74	0.028	280
LLDPE-Pd	0.70	16.6	0.27	61
LLDPE-Pd/LDPE (30/70)microlayer	0.21	16.1	0.77	21
PET-Pd (amorphous)	0.76	0.34	0.0046	80
Nylon 6,6-Pd	0.36	0.041	0	
Nylon 6,6	0.00	0.086	0.070	

[a] P, cm^3[STP] cm m^{-2} atm^{-1} day^{-1}.

TABLE IV
Effect of Oxygen Pressure on Oxygen Transport Properties of Pd-Infused Polymers[a]

Material	Metal content (wt %)	100% O_2			Air		
		P_1 (N_2 purge)	P_2 (N_2 + 2%H_2 purge)	P_1/P_2	P_3 (N_2 purge)	P_4 (N_2 + 2%H_2 purge)	P_3/P_4
FEP-1X Pd	0.41	17.1	0.133	130	18.9	0.016	1100
FEP-5X Pd	0.83	15.2	0.097	160	12.6	0.021	600
PP-Pd	0.29	7.74	0.028	280	6.60	0.010	660
LLDPE-Pd	0.70	16.6	0.027	610	17.1	0.033	520
PET-Pd	0.76	0.34	0.0047	70	—	—	—

[a] P, cm^3[STP] cm m^{-2} atm^{-1} day^{-1}.

References

1. Alivisatos, A. P. Science 1996, 271, 933.
2. Shipway, A. N.; Katz, E.; Willner, I. Chem Phys 2000, 1, 18.
3. Lewis, L. N. Chem Rev 1993, 93, 2693.
4. McEuen, P. L. Science 1997, 278, 1729.
5. Ma, S. K.; Lue, J. T. Solid State Commun 1996, 97, 979.
6. Gangopadhyay, R.; De, A. Chem Mater 2000, 12, 608.
7. Dabbousi, B. O.; Bawendi, M. G.; Onitsuka, O.; Tybner, M. F. Appl Phys Lett 1995, 66, 1316.
8. Coronado, E.; Galan-Mascaros, J. R.; Gomez-Garcia, C. J.; Laukhin, V. Nature 2000, 408, 447.
9. Wang, Y.; Herron, N. Science 1996, 273, 632.
10. Winiarz, J. G.; Zhang, L. M.; Lai, M.; Friend, C. S.; Prasad, P. N. J Am Chem Soc 2001, 123, 10502.
11. Sidorov, S. N.; Volkov, I. V.; Davankov, V. A. J Am Chem Soc 2001, 123, 10502.
12. Pinnavaia, T. J. Science 1983, 220, 365.
13. Merkel, T. C.; Freeman, B. D.; Spontak, R. J.; He, Z.; Pinnau, I.; Meakin, P.; Hill, A. J. Science 2002, 296, 519.
14. Shiflett, M. B.; Foley, H. C. Science 1999, 285, 1902.
15. Galow, T. H.; Drechsler, U.; Hanson, J. A.; Rotello, V. M. Chem Commun 2002, 10, 1076.
16. Reynaud, E.; Gauthier, C.; Perez, J. Rev Metall 1999, 2, 169.
17. Wu, C. L.; Zhang, M. Q.; Rong, M. Z.; Friedrich, K. Compos Sci Technol 2002, 62, 1327.
18. Sumita, M.; Tsukumo, Y.; Miyasaka, K.; Ishikawa, K. J Mater Sci 1983, 18, 1758.
19. Jana, S. C.; Jain, S. Polymer 2001, 42, 6897.
20. Rong, M. Z.; Zhang, M. Q.; Zheng, Y. X.; Zeng, H. M.; Walter, R.; Friedrich, K. Polymer 2001, 42, 167.
21. Sellinger, A.; Weiss, P.; Nguyen, A.; Lu, Y.; Assink, R. A.; Gong, W.; Brinker, C. J. Nature 1998, 394, 256.
22. Vargo, T. G.; Koloski, T. S. Fabrication of Metal-Oxide Macromolecular Networks within Fluoropolymer Free Volume, Proceedings of Fluorine in Coatings III, Paper #38, Paint Research Council, Orlando, FL, Jan. 25–27, 1999.
23. Koloski, T. S.; Vargo, T. G. U.S. Pat. 5,977,241, 1999.
24. Vargo, T. G.; Koloski, T. S. U.S. Pat. 6,232,386, 2001.
25. Sekelik, D. J.; Stepanov, S. V.; Nazarenko, S.; Schiraldi, D.; Hiltner, A.; Baer, E. J Polym Sci Part B: Polym Phys 1999, 37, 847.
26. Lewis, F. A. The Palladium-Hydrogen System; Academic Press: London, 1967.
27. Nowakowski, R.; Grzeszczak, P. R. Dus Surf Sci 2002, 813, 507.
28. Mitsui, T.; Rose, M. K.; Fomin, E.; Ogletree, D. F.; Salmeron, M. Surf Sci 2002, 259, 511.
29. Engle, T.; Kuipers, H. Surf Sci 1979, 181, 90.